Available online at www.sciencedirect.com

ScienceDirect

Procedia Structural Integrity 12 (2018) 58–70

Structural Integrity Procedia

www.elsevier.com/locate/procedia

AIAS 2018 International Conference on Stress Analysis

On the DMT adhesion theory: from the first studies to the modern applications in rough contacts

Guido Violano[a], Giuseppe Pompeo Demelio[a], Luciano Afferrante[a,*]

[a]*Department of Mechanics, Mathematics and Management, Politecnico of Bari, V.le Japigia, 182, 70126, Bari, Italy*

Abstract

In the last years, increasing interest has been devoted to the study of the adhesion between rough media. The Derjaguin, Muller & Toporov (DMT) theory is one of the most known models to describe adhesion between hard elastic solids with long range adhesive interactions. However, many versions of the DMT theory can be found in the literature.

In the first part of the present work, we try to make order about the various versions of the DMT theory appeared over the years. All models, often confusedly called with the same name "DMT theory", are based on the same assumption of neglecting deformations due to the adhesive forces. They predicts the same value of the detachment force at the pull-off, but only the so-called DMT force approach correctly captures the evolution trend of the adhesive force during the contact.

In the second part of the work, we address the problem to include adhesion in the contact of rough surfaces according to the DMT theory. Specifically, we compare the Maugis' idea to add adhesion in the Greenwood and Williamson asperity theory, with more recent models: the *Interacting and Coalescing Hertzian Asperities* (ICHA) one and the Persson's theory. The two models, which both take account of adhesion according to the DMT force approach, give very similar results, showing that the pull-off force is negligibly affected by the shortest wavelength components of the surface roughness.

On the contrary, the Maugis' model strongly underestimates adhesion and predicts a vanishing pull-off force when the upper cut-off spatial frequency of the surface is increased.

Keywords: DMT theory; fractal surfaces; roughness; adhesion.

1. Introduction

The first study of adhesion between bodies is due to Bradley (1932), which integrated the Lennard-Jones interaction law between rigid spheres finding a total attractive force equal to $2\pi\Delta\gamma R$, where $\Delta\gamma$ is the adhesion surface energy and R is the composite radius of the contacting spheres. In order to study the adhesive contact between elastic spheres, Derjaguin (1934) supposed deformations of the contacting bodies are not affected by attractive interactions, and hence

* Corresponding author. Tel.: +39 080 5962704.
E-mail address: luciano.afferrante@poliba.it

10.1016/j.prostr.2018.11.106

he assumed a Hertzian gap between the deformed spheres. He found the detachment occurs at zero contact area with a pull-off force $\pi\Delta\gamma R$.

In the same work, Derjaguin computed the attractive force acting between a sphere and a plane separated by a "small" positive gap. In this case, he obtained an attractive force equal to the value calculated by Bradley (1932). Derjaguin supposed the adhesive force between a sphere and a plane is proportional to the interaction potential between flat surfaces at the same distance (*Derjaguin approximation*). Such a condition is valid if one assumes that the attractive forces do not modify the surfaces profile (Barthel (2008)). This assumption is also at the basis of the so-called *DMT theory* proposed by Derjaguin, Muller & Toporov.

Specifically, in 1975, they presented a first version of their theory (Derjaguin et al. (1975)), where the adhesive force between an elastic sphere and a flat layer is calculated by computing the rate of change of the surface energy as the penetration of the sphere is increased. Such approach (formally known as *DMT thermodynamic approach*) predicts a pull-off force equal to $2\pi\Delta\gamma R$. Moreover, the detachment occurs at zero penetration and the adhesive load decreases as the penetration increases.

An improved version of the DMT theory was presented by Muller et al. (1983). Actually, in this second version, the authors introduced two different methods to calculate the adhesive force. The first one is again the thermodynamic approach, but with a more accurate law of interaction. The second method is the so-called *DMT force approach*, according to which the adhesive load is computed by summing up the adhesive interactions outside the contact area. This approach leads to a pull-off force still equal to $2\pi\Delta\gamma R$, but this time the adhesive force is an increasing function of the penetration in agreement with previous numerical calculations performed by Muller et al. (1980).

Really, results of the DMT theory appeared at first to be contradictory with respect to the predictions of the Johnson, Kendall & Roberts (JKR) theory (Johnson et al. (1971)). The JKR theory assumes interaction is fully characterized by the work of adhesion $\Delta\gamma$ (the spatial extent of the wall-wall interaction potential is neglected) and considers the effect of adhesion only inside the area of contact. Finally, the solution is found by a balance between the stored elastic energy and the loss in surface energy. In the JKR theory the force at pull-off is found to be $1.5\pi\Delta\gamma R$.

Tabor (1977), showed that the two theories applied to opposite extremes of a spectrum of the parameter (known as Tabor parameter) $\mu = \left[R\Delta\gamma^2/\left(E^{*2}z_0^3\right)\right]^{1/3}$, where E^* is the composite elastic modulus of the spheres and z_0 is the equilibrium separation, which is of the order of magnitude of the interatomic distance. Such a parameter represents the ratio between the displacements of the spheres at the pull-off and the range of surfaces characterized by z_0.

The DMT theory applies at low values of μ, i.e. for small, rigid spheres and long range interactions. The JKR theory is instead more appropriate at large values of μ, i.e. for large, compliant spheres and short range interactions. In particular, Pashley (1984) and Greenwood (2007) gave the value of 0.24 as upper limit for applicability of the DMT force approach. Moreover, Muller et al. (1980), Greenwood (1997), Feng (2000) and Feng (2001) showed that the effective value of the pull-off force is always lower than $2\pi\Delta\gamma R$, moving towards $1.5\pi\Delta\gamma R$ at high μ.

Several works showed that surface roughness strongly affects adhesion (Fuller & Tabor (1975), Cheng et al. (2002), Wei et al. (2010), Ramakrishna et al. (2013), Jacobs et al. (2013), Afferrante et al. (2015)). In this respect, many efforts have been done with the aim of extending the adhesion theories for smooth contacts to rough ones.

Maugis (1996), for example, extended the multiasperity theory of Greenwood & Williamson (1966) (GW) to the DMT case. In the GW theory, roughness is modeled by a set of spherical identical asperities, whose heights follow a well defined statistical distribution. According to the Maugis idea, adhesion is added to the GW model by adjusting the load due to each asperity in contact. Specifically, the load is computed by subtracting to the Hertzian contribution an adhesive constant term equal to $2\pi\Delta\gamma R$. Frequently, the Maugis approximation has been denoted as the real DMT theory. Actually, the Maugis idea of taking the adhesive term to be constant, can be considered as an alternative DMT model (which we identify with the acronym DMT-M).

More recently, Persson & Scaraggi (2014) (PS) implemented the DMT force approach in the Persson's theory. They found a good agreement between numerical simulations and analytical predictions.

Pastewka & Robbins (2014) (PR) presented a criterion for adhesion between rough surfaces. In the calculations of the attractive force, PR assumed that the variation of the surface separation is not affected by adhesion. This is the classical approximation found in the DMT theory. The PR criterion suggests a strong dependence of the pull-off force on the slopes and the curvatures that characterize the surface topography. However, this is in contrast with the *bearing area model* (BAM) proposed by Ciavarella (2018), where the attractive area is estimated from the bearing area and the force of attraction is computed by assuming a Maugis-Dugdale potential (Maugis (1992)) acting between the bodies.

Specifically, the BAM shows a negligible effect of the slopes and curvatures on the pull-off force, especially at low fractal dimensions.

Very recently, the *Interacting and Coalescing Hertzian Asperities* (ICHA) model, which showed to be very accurate in predicting the contact quantities in problems with contacting rough surfaces ((Afferrante et al. (2012), Afferrante et al. (2018), Muser et al. (2017)), has been extended to include adhesion in the framework of the DMT theory (Violano et al. (2018), Violano & Afferrante (2018)).

In this paper we present a review on the various DMT models. In the first part of the work, the mathematical formulation of the different DMT approaches is presented, with applications to the simple case of spherical contact. In the second part of the work, adhesive rough contact models based on the DMT theory are compared.

2. Contact of spheres

2.1. The Derjaguin model

Derjaguin (1934) extended the Hertz contact theory for elastic spheres to the adhesive case. He calculated the applied force as the derivative of the total energy of the system with respect to the penetration δ. Specifically, under the assumption that attractive interactions do not deform the bodies, the penetration δ and the contact force F are given by

$$\delta = \frac{a^2}{R}, \tag{1}$$

$$F = F_H - F_{ad} = \frac{4}{3}E^* \frac{a^3}{R} - \pi\Delta\gamma R, \tag{2}$$

where E^* is the composite elastic modulus of the materials, $R = R_1R_2/(R_1 + R_2)$ is an equivalent radius, a is the radius of contact and $\Delta\gamma$ is the adhesion surface energy.

In such formulation, the adhesive load $F_{ad} = \pi\Delta\gamma R$ is constant and depends only on the surface energy. The detachment occurs at $a = 0$ (i.e. $\delta = 0$) with a pull-off force equal to $\pi\Delta\gamma R$.

2.2. The DMT thermodynamic approach (DMT-T)

The first version of the DMT theory was published in 1975 (Derjaguin et al. (1975)). Differently from the original paper (Derjaguin (1934)), the authors proposed a new definition of the surface energy

$$W_{ad} = \pi\Delta\gamma a^2 + 2\pi \int_a^\infty \Gamma(u(r,\delta))rdr, \tag{3}$$

taking account of both the contribution inside the contact area ($\pi\Delta\gamma a^2$) and the adhesive interactions outside the contact zone ($2\pi \int_a^\infty \Gamma\left[u(r,\delta)\right] rdr$) . $\Gamma\left[u(r,\delta)\right]$ is the interatomic potential depending on the radial coordinate r and penetration δ, through the Hertzian gap

$$u(r,\delta) = \frac{1}{\pi R}\left[R\delta\sqrt{\frac{r^2}{R\delta} - 1} - \left(2R\delta - r^2\right)\arctan\sqrt{\frac{r^2}{R\delta} - 1}\right] \tag{4}$$

The adhesive force is hence calculated by deriving the potential W_{ad} with respect to the approach δ

$$F_{ad} = \frac{dW_{ad}}{d\delta} = \pi\Delta\gamma R + 2\pi \int_a^\infty \frac{d\Gamma(u)}{du}\frac{du(r,\delta)}{d\delta}rdr, \tag{5}$$

where

$$\frac{d\Gamma(u)}{du} = \frac{2\Delta\gamma}{\varepsilon}\left(\frac{\varepsilon}{u+\varepsilon}\right)^3 \tag{6}$$

and ε is the range of attractive forces, whose value is of the order of magnitude of the atomic spacing z_0

Detachment still occurs at zero contact area and for a pull-off force equal to $2\pi\Delta\gamma R$, which is twice the value originally obtained by Derjaguin (1934).

2.3. The improved DMT thermodynamic approach (IDMT-T)

Muller et al. (1983) improved their original thermodynamic approach by describing the adhesive interactions with a two-term Lennard-Jones potential law. As a result, eq. (6) becomes

$$\frac{d\Gamma(u)}{du} = \frac{8\Delta\gamma}{3\varepsilon}\left[\left(\frac{\varepsilon}{u+\varepsilon}\right)^3 - \left(\frac{\varepsilon}{u+\varepsilon}\right)^9\right], \tag{7}$$

giving an adhesive force decreasing with the penetration.

2.4. The DMT force approach (DMT-F)

In the same work, Muller et al. (1983) proposed an alternative method to calculate the adhesive force by summing up the adhesive interactions acting outside the contact zone

$$F_{ad} = 2\pi\int_a^\infty \frac{8\Delta\gamma}{3\varepsilon}\left[\left(\frac{\varepsilon}{u(r,\delta)+\varepsilon}\right)^3 - \left(\frac{\varepsilon}{u(r,\delta)+\varepsilon}\right)^9\right] rdr. \tag{8}$$

Pull-off still occurs at a force $2\pi\Delta\gamma R$, but, in such case, the adhesive force is found to be an increasing function of the penetration.

2.5. The Maugis approximation of the DMT theory (DMT-M)

To solve the contradiction between the thermodynamic and force approach, Maugis (1992) proposed to consider a constant adhesive contribution $F_{ad} = 2\pi\Delta\gamma R$ independent of the indentation of the sphere.

2.6. Discussion

The above summarized models move from the same assumption: a Hertzian gap profile is assumed, thus neglecting the effect of adhesive interactions on the displacements. Despite this common starting idea, the various models are based on a different computation of the adhesive force.

Fig. 1 shows the adhesive load F_{ad}, normalized with respect to the quantity $2\pi\Delta\gamma R$, as a function of the ratio a/R. Calculations have been performed at $\mu = 0.2$.

The thermodynamic approaches DMT-T and IDMT-T give very close results, with an adhesive force confined between the values predicted by the original Derjaguin model and Maugis approximation (DMT-M model). In particular, the adhesive force decreases asymptotically from $2\pi\Delta\gamma R$ (pull-off force) towards $\pi\Delta\gamma R$ for high values of the contact radius (i.e. high penetrations).

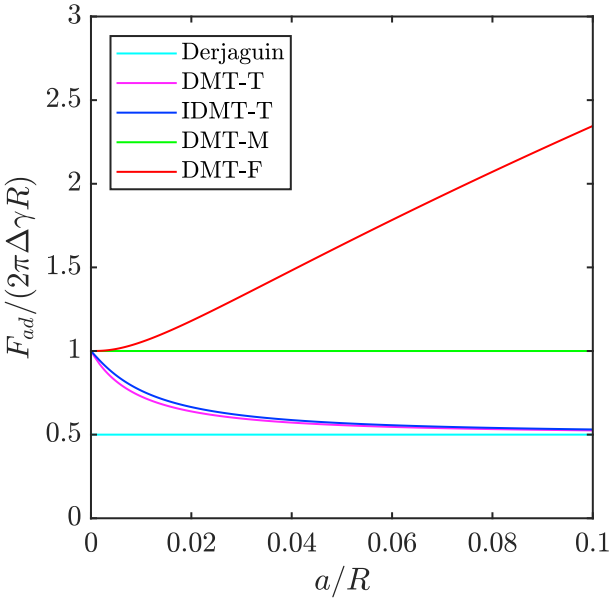

Fig. 1. The normalized adhesive force $F_{ad}/(2\pi\Delta\gamma R)$ as a function of the ratio a/R. Results are referred to: i) Derjaguin model (cyan); ii) DMT thermodynamic approach (magenta); iii) improved DMT thermodynamic approach (blue); iv) DMT-Maugis model (green); v) DMT force approach (red). Calculations are performed at $\mu = 0.2$.

On the contrary, the DMT-F approach predicts an adhesive force increasing with the contact area. Really, as observed by Pashley (1984), thermodynamic and force approach should give the same results. However, this is not the case because the deformed profile does not correspond to an effective equilibrium configuration at a minimum point of the energy. In fact, the deformed profile is arbitrarily determined with the assumption to follow the Hertzian prediction.

The force method is however the only approach giving the correct relationship between adhesive force and contact area, as observed by Muller et al. (1983) and Pashley (1984).

Similar conclusions can be drawn from Fig. 2, where the normalized applied force $F/2\pi\Delta\gamma R$ is plotted in terms of the ratio δ/ε. Numerical results presented by Greenwood (2007) are also plotted as reference. At negative penetrations (i.e. positive gap), the problem is governed by the Bradley's solution, as in the DMT theory adhesive interactions are assumed not to deform the bodies. In the range of positive penetrations, the thermodynamic approaches give larger values of the applied load as a result of the erroneous computation of the adhesive load. Notice, in such range, the very simple approximation of Maugis works better.

3. Contact of rough bodies

Adhesion is of wide interest in many fields, e.g. nano-mechanics (He et al. (2018), Menga et al. (2016)), biomimetics (Afferrante & Carbone (2012), Afferrante & Carbone (2013), Dening et al. (2014)), electronics (Hoang et al. (2017), Rauscher et al. (2018)). Several works investigated the effect of roughness on adhesion, which significantly affects the contact solution also at the micro- and nano-scale (Pastewka & Robbins (2014)).

In this section, we review some of the most known theories implementing the DMT approach to study the adhesive contact of randomly rough surfaces.

3.1. Maugis extension of the Greenwood & Williamson model to DMT contacts (GW-M model)

Maugis (1996) extended the GW multiasperity model by introducing adhesion according to his approximation of considering the adhesive force independent of the penetration. In the GW model, roughness is replaced by spherical asperities, all having the same radius of curvature R. The contact solution is obtained independently for each asperity,

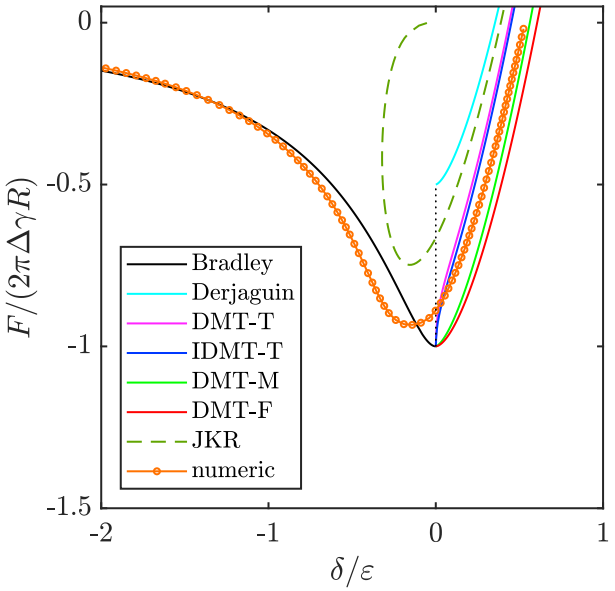

Fig. 2. The normalized applied force $F/(2\pi\Delta\gamma R)$ as a function of the dimensionless penetration δ/ε. Results are referred to: i) Bradley model (black); ii) Derjaguin model (cyan); iii) DMT thermodynamic approach (magenta); iv) improved DMT thermodynamic approach (blue); v) DMT-Maugis model (green); vi) DMT force approach (red); vii) JKR theory (green dashed line); viii) numerical solution (orange line with circular markers). Calculations are performed at $\mu = 0.2$.

thus neglecting the elastic coupling of the contact regions. In particular, denoting with $\bar{d}$ the distance between the plane of summits and the smooth plane and with $\varphi(z)$ the heights distribution of asperities, the number of asperities in contact n_c can be written as

$$n_c = n_{tot} \int_{\bar{d}}^{\infty} \varphi(z) dz, \tag{9}$$

where n_{tot} is the total number of the summits.

The total real area and total load are obtained by summing the Hertzian relations $A_i = \pi R\left(z_i - \bar{d}\right)$ and $F_i = 4E^* R^{1/2}\left(z_i - \bar{d}\right)^{3/2}/3$ obtained on the ith sphere, for all the asperities in contact

$$A = n_{tot} \int_{\bar{d}}^{\infty} A_i \varphi(z)\, dz \tag{10}$$

$$F = n_{tot} \int_{\bar{d}}^{\infty} F_i \varphi(z)\, dz \tag{11}$$

In presence of adhesion and according to the Maugis' approximation for contacts of the DMT type, the calculations of n_c and A are not modified, but for F we have

$$\begin{aligned} F &= n_{tot} \int_{\bar{d}}^{\infty} \left(4E^* R^{1/2}\left(z_i - \bar{d}\right)^{3/2}/3 - 2\pi\Delta\gamma R\right)\varphi(z)\, dz \\ &= \frac{4}{3} n_{tot} E^* R^{1/2} \int_{\bar{d}}^{\infty} \left(z_i - \bar{d}\right)^{3/2} \varphi(z)\, dz - 2\pi\Delta\gamma R n_c \end{aligned} \tag{12}$$

Therefore, the total adhesive load $F_{ad} = 2\pi\Delta\gamma R n_c$ is simply the sum of the constant adhesive contribution calculated for each asperity in contact.

3.2. Interacting and Coalescing Hertzian Asperities (ICHA) model

The ICHA model, presented for the first time by Afferrante et al. (2012), can be classified in the category of mixed asperity-BEM models. As in the classical multiasperity models, the real surface is replaced with parabolic asperities with radii of curvature equal to the geometric mean of the principal radii (Greenwood (2006)). Elastic coupling between contact regions is considered by following the procedure proposed by Ciavarella et al. (2006) and successively improved by Afferrante et al. (2018). Specifically, the displacement at a distance r from the location of a certain asperity is calculated by using the Johnson's formulas (Johnson (1985)) of an elastic half-space in contact with a single axisymmetric parabolic asperity. Thus, the total displacement at the location of the i^{th} asperity is calculated by summing up the contribution for all the asperities in contact

$$\begin{aligned} w_i &= \frac{a_i^2}{R_i} + \sum_{j=1,j\neq i}^{n_c}\left(\frac{a_j^2}{R_j} - \frac{r_{ij}^2}{2R_j}\right) && \text{if } r_{ij} < a_j \\ w_i &= \frac{a_i^2}{R_i} + \frac{1}{\pi}\sum_{j=1,j\neq i}^{n_c}\left(\frac{2a_j^2 - r_{ij}}{R_j}\arcsin\frac{a_i}{r_{ij}} + \frac{a_j}{R_j}\sqrt{r_{ij}^2 - a_j^2}\right) && \text{if } r_{ij} \geq a_j \end{aligned} \tag{13}$$

where r_{ij} is the distance between the asperities i and j.

Moreover, when the applied load is increased, the number of asperities in contact increases and adjacent asperities can merge to form larger contact regions. To take account of this phenomenon, overlapping contact asperities are replaced with an equivalent one, which preserves the total area of contact and the geometric volume centroid.

Adhesion is introduced in the model according to the DMT-F approach, i.e. by assuming displacements are not modified by adhesive interactions. Under such assumption, the total adhesive force can be calculated as (see Persson & Scaraggi (2014), Violano et al. (2018))

$$\begin{aligned} F_{ad} &= A_0 \int_{A_{nc}} \frac{d\Gamma\left[u\left(\mathbf{x}\right)\right]}{du} dA \\ &= A_0 \int_0^{\infty} \frac{d\Gamma\left[u\left(\mathbf{x}\right)\right]}{du} P(u) du \end{aligned} \tag{14}$$

where $d\Gamma\left[u\left(\mathbf{x}\right)\right]/du$ is given by eq. (7), A_{nc} is the non-contact area, A_0 is the nominal contact area and $P(u)$ is the gap probability distribution.

3.3. Persson's theory

Persson (2001) developed an innovative multiscale theory for the contact mechanics of rough surfaces. In the original formulation of the theory, the contact between a flat elastic half-space and a rough rigid surface is studied assuming equal the power spectral densities (PSD) of the deformed half-space and rigid surface. Such assumption, which is rigorously true in full-contact conditions, leads to less and less accurate results moving towards small loads (i.e. large separations).

For this reason, Persson (2008) proposed an improvement of his theory by adjusting the PSD of the deformed half-space in partial contact with a corrective factor $S\left(q\right) = \gamma + \left(1-\gamma\right)\left[A\left(q\right)/A_0\right]^2$, where $q = |\mathbf{q}|$ is the modulus of the wave vector $\mathbf{q}$ and γ is an empirical parameter whose value can be taken in the range $0.4 - 0.5$. With this correction, the contact area at the applied load F can be expressed as

$$\frac{A}{A_0} = \operatorname{erf}\left(\frac{F}{A_0\sqrt{\left\langle\nabla u^2\right\rangle/2}E^*}\right) \tag{15}$$

where $\langle\cdot\rangle$ is the ensemble average operator and $\left\langle\nabla u^2\right\rangle = \int_{q_L}^{q_1} d^2q\, q^2 C\left(\mathbf{q}\right) S\left(q\right)$ can be interpreted as the averaged square slope of the deformed half-space (we have denoted with $C\left(\mathbf{q}\right)$ the PSD of the rigid rough surface).

For contacts of the DMT type, adhesion can be introduced in the Persson's theory by computing the adhesive force according to eq. (14) (see Persson & Scaraggi (2014)).

In this work, about the gap probability distribution $P(u)$, we have used a more accurate expression, as given in Afferrante et al.(2018), with respect to the formulation proposed by Almqvist et al. (2011). Therefore, denoting with ζ the magnification, $P(u)$ writes as

$$P(u) \approx \frac{1}{A_0}\int d\zeta \frac{-(dA(\zeta)/d\zeta)}{(2\pi h^2_{\mathrm{rms}_{\mathrm{eff}}}(\zeta))^{1/2}} \times \left[\exp\left(-\frac{(u-u_1(\zeta))^2}{2h^2_{\mathrm{rms}_{\mathrm{eff}}}(\zeta)}\right) + \exp\left(-\frac{(u+u_1(\zeta))^2}{2h^2_{\mathrm{rms}_{\mathrm{eff}}}(\zeta)}\right)\right], \tag{16}$$

where $h_{\mathrm{rms}_{\mathrm{eff}}}(\zeta) = \left[h^{-2}_{\mathrm{rms}}(\zeta) + u_1^{-2}(\zeta)\right]^{-1/2}$, being $h^2_{\mathrm{rms}}(\zeta) = \int_{q>q_0\zeta} d^2q\, C(\mathbf{q})$. Moreover $u_1(\zeta)$ is the average separation in the surface area that moves out of contact when the magnification is increased of an infinitesimal quantity $d\zeta$, and can be calculated as (see Yang & Persson (2008))

$$u_1(\zeta) = \bar{u}(\zeta) + \left[(d\bar{u}(\zeta)/d\zeta)A(\zeta)\right]/(dA(\zeta)/d\zeta) \tag{17}$$

where $\bar{u}(\zeta)$ is the mean interfacial separation, which is given by (see Yang & Persson (2008))

$$\bar{u}(\zeta) = \frac{1}{2\sqrt{\pi}}\int_{D(\zeta)} d^2q\, qC(\mathbf{q})\, w(q) \int_{\sigma_0}^{\infty} \frac{d\sigma}{\sigma}\left[\gamma + 3(1-\gamma)\,\mathrm{erf}^2\left(\frac{w(q)\,\sigma}{E^*}\right)\right] e^{-\left(\frac{w(q)\sigma}{E^*}\right)^2} \tag{18}$$

where $D(\zeta) = \{\mathbf{q} \in \mathbb{R}^2 |\, q_L \le |\mathbf{q}| \le \zeta q_L\}$, and

$$w(q) = \left(\frac{1}{2}\int_{D_q} d^2q'\, q'^2 C(\mathbf{q}')\right)^{-1/2} \tag{19}$$

being $D_q = \{\mathbf{q} \in \mathbb{R}^2 |\, q_L \le |\mathbf{q}| \le q\}$.

3.4. Discussion

Calculations with the ICHA model and Persson's theory are performed on self-affine fractal surfaces with PSD described by a power law

$$C(\mathbf{q}) = \begin{cases} C_0 & \text{if } q_L \le |\mathbf{q}| \le q_0 \\ C_0 q^{-2(H+1)} & \text{if } q_0 \le |\mathbf{q}| \le q_1 \end{cases}, \tag{20}$$

where H is the Hurst exponent and $\mathbf{q}$ is the wave vector, being $q = |\mathbf{q}|$. The quantities q_L and q_1 are the lower and upper cut-off wave vectors, while q_0 is the crossover wave vector from the power law $C_0 q^{-2(H+1)}$ for $q > q_0$ to the constant C_0 for $q < q_0$ (also known as roll-off wave vector). Specifically, the fractal surface are numerically generated by exploiting the spectral method developed in Putignano et al. (2012) with a fixed root mean square (rms) roughness amplitude $h_{\mathrm{rms}} = 0.52$ nm. Moreover, the short cut-off spatial frequency q_L is fixed to 2.5×10^{-5} m^{-1}, and $q_0 = 4q_L$.

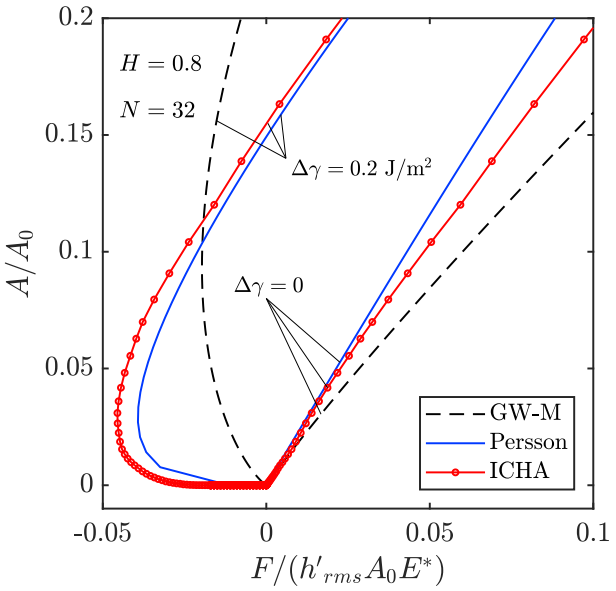

Fig. 3. The relative contact area A/A_0 as a function of the applied load $F/(A_0E^*h'_{\rm rms})$. ICHA model results are plotted with red markers, the Persson's theory ones with blue solid line, the GW-M model ones with black dashed line. Calculations are performed in presence ($\Delta\gamma = 0.2$ J/m^2) and absence ($\Delta\gamma = 0$) of adhesion on a surface with $N = 32$ and $H = 0.8$.

Calculations with the GW-M model are instead performed by considering a Gaussian height distribution of circular asperities with radius equal to the average curvature radius $\bar{R} = 2/h''_{\rm rms}$ of the generated fractal surfaces (where $h''_{\rm rms} = \left[\left\langle\left(\nabla^2 h\right)^2\right\rangle\right]^{1/2}$), and standard deviation equal to the root mean square (rms) roughness amplitude $h_{\rm rms}$.

In all simulations, we have assumed $E^* = 1.33 \cdot 10^{12}$ Pa and $\Delta\gamma = 0.2$ J/m^2. The attractive range of adhesive interactions ε has been fixed to 1 nm.

Fig. 3 shows the area-load relation in presence and absence of adhesion. Calculations have been performed on a surface with $H = 0.8$ and $N = 32$. The curves predicted by the GW-M model (black dashed line) significantly deviate from the ICHA model (red line with circular markers) and Persson's theory (blue line), which instead are in very good agreement. In absence of adhesion, as expected, in the range of small contact areas the area-load relation is linear. However, in such case, the ICHA model correctly predicts the coefficient of proportionality κ ($\kappa \sim 2$), while the Persson's theory slightly overestimate it ($\kappa \approx 2.15$). On the contrary, at high loads, close to complete contact, the Persson's theory is expected works well.

Figs. 4 and 5 investigate the effect of fractal dimension $D = 3 - H$ and number of scales on the contact behavior. Specifically, in Fig. 4 calculations are performed on surfaces with $N = 64$ and $H = 0.4, 0.6, 0.8$, while in fig. 5 on surfaces with $H = 0.8$ and $N = 16, 32, 64$.

At fixed load, the contact area increases with the Hurst exponent H, as the size of the contact spots reduces because of the shrinking of the asperities radii of curvature. The effect of increasing N is instead opposite, with the relative area which reduces when the number of scales grows. In such case, indeed, the contact is splitted in several microspots and the resulting contact area is smaller.

In the DMT limit, adhesive hysteresis is neglected and this is effectively observed when we deal with hard solids and low surface energy (see Pastewka & Robbins (2014), Medina & Dini (2014)). The pull-off force can be hence assumed equal to the maximum tensile load reached during the loading phase.

Fig. **??** shows the normalized pull-off force as a function of the Fuller & Tabor (FT) adhesive parameter $\theta_{FT} = E^* h_{\rm rms}^{3/2} \bar{R}^{1/2} / \left(\Delta\gamma \bar{R}\right)$. The parameter θ_{FT} represents the ratio between the compressive repulsive force and the tensile adhesive one. When θ_{FT} increases a reduction of the detachment force is then expected. Results in fig. **??** are obtained at different values of the number of scales ($N = 16, 32, 64$) and Hurst exponent ($H = 0.4, 0.6, 0.8$). The symbols size decreases at higher values of N, while the shape of the symbols depends on the value of H, as specified in the figure

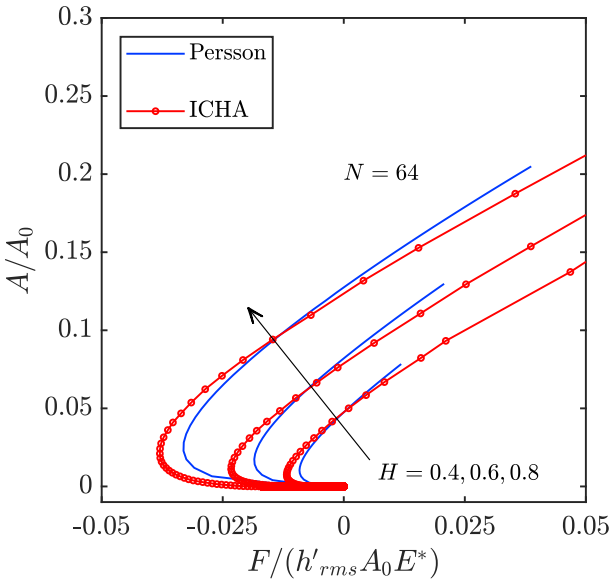

Fig. 4. The relative contact area A/A_0 as a function of the applied load $F/(A_0E^*h'_{\rm rms})$. ICHA model results are plotted with red markers, the Persson's theory ones with blue solid line. Calculations are performed on surfaces with $N = 64$ and $H = 0.4, 0.6, 0.8$. The surface energy is $\Delta\gamma = 0.2$ J/m^2.

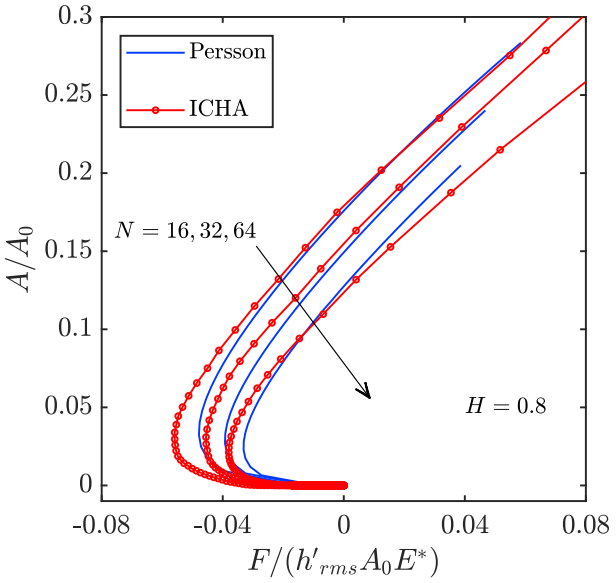

Fig. 5. The relative contact area A/A_0 as a function of the applied load $F/(A_0E^*h'_{\rm rms})$. ICHA model results are plotted with red markers, the Persson's theory ones with blue solid line. Calculations are performed on surfaces with $H = 0.8$ and $N = 16, 32, 64$. The surface energy is $\Delta\gamma = 0.2$ J/m^2.

caption. ICHA model (red symbols) and Persson's theory (blue symbols) predicts the same trend for the pull-off force even if the Persson's theory leads to slightly lower values.

The slight decrease of the pull-off force with decreasing H can be easily justified by observing that a reduction in H entails a decrease in the mean curvature radius $\bar{R}$, and then an increase in θ_{FT}. For the same reason, an increase in the number of scales determines a decrease of the detachment force, even if the influence of N on the pull-off force is less and less significant as N increases. This is in agreement with the recent results given in Joe et al. (2017), where

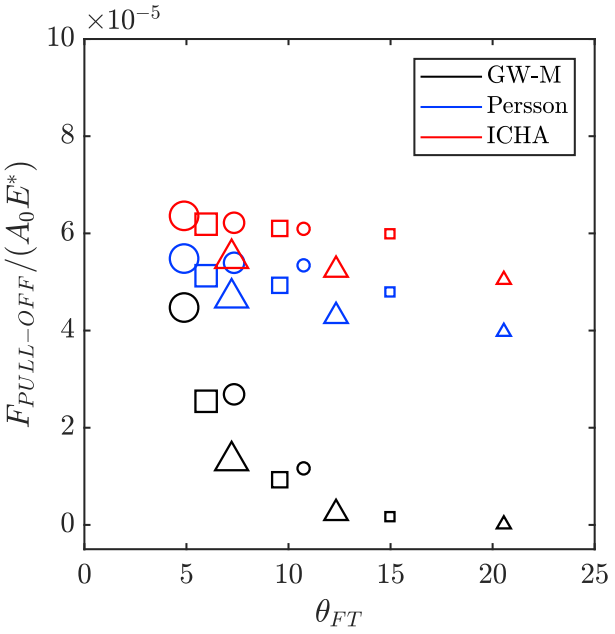

Fig. 6. The normalized pull-off force as a function of the FT adhesion parameter θ_{FT}. ICHA model results are plotted with red markers, the Persson's theory ones with blue markers and the GW-M model ones with black markers. Calculations are performed on surfaces with $H = 0, 4$ (triangles), $H = 0.6$ (squares) and $H = 0.8$ (circles) and at different number of scales ($N = 16, 32, 64$). The symbol size decreases as N increasing.

the adhesive contact of rough surfaces is studied at increasing cut-off frequency q_1. It is found that the contact solution (in terms of a modified interfacial force) converges at arbitrarily large wavenumbers.

The predictions of the GW-M theory (black symbols) strongly underestimates the effect of adhesion on the force required to detach the bodies. This is particularly evident at the higher values of the FT parameter.

4. Conclusions

The adhesion of elastic bodies has attracted a lot of interest in the past years. Here, we have tried to make order about the historical evolution of the so-called DMT theory. In the first part of the work, we recall the various formulations appeared in the literature over the years. Although the various approaches move from the same assumptions that adhesion act only outside the contact area and adhesive interactions do not deform the bodies, they lead to different results. In particular, with reference to the contact between spherical bodies, all models predicts the same pull-off force $2\pi R\Delta\gamma$, but only the DMT force approach gives also the correct trend between adhesive force and penetration (or contact area).

In the second part of the work, we discuss about the application of the DMT theory to the contact of rough surfaces. Specifically, we have considered: (i) the Maugis' extension of the classical GW multiasperity theory (GW-M), based on the idea of taking constant the adhesive force on each asperity in contact, (ii) the application of the DMT force approach to a recent advanced version of the Persson's theory, and (iii) a new advanced multiasperity model (the ICHA model) including adhesion in accordance with the DMT force approach. The ICHA model and Persson's theory predictions are in very good agreement. On the contrary, significant discrepancies are observed with the GW-M theory.

In our calculations, we found that the pull-off force decreases at higher fractal dimensions, while the effect of the number of scales on the detachment force is almost negligible. This is in agreement with recent findings showing that the interfacial adhesive force is almost insensitive to the upper cut-off spatial frequency q_1 of the surface, provide that q_1 is sufficiently large.

References

Afferrante, L., & Carbone, G., 2012. Biomimetic surfaces with controlled direction-dependent adhesion. Journal of The Royal Society Interface, 9(77), 3359–3365.

Afferrante, L., Carbone, G., & Demelio, G., 2012. Interacting and coalescing Hertzian asperities: A new multiasperity contact model. Wear, 278–279, 28–33.

Afferrante, L., & Carbone, G., 2013. The mechanisms of detachment of mushroom-shaped micro-pillars: From defect propagation to membrane peeling. Macromolecular Reaction Engineering, 7(11), 609–615.

Afferrante, L., Ciavarella, M., & Demelio, G., 2015. Adhesive contact of the Weierstrass profile.Proceedings of the Royal Society A: Mathematical, Physical and Engineering Sciences.471 (2182), Art. no. 20150248.

Afferrante, L., Bottiglione, F., Putignano, C., Persson, B. N. J., & Carbone, G., 2018. Elastic Contact Mechanics of Randomly Rough Surfaces: An Assessment of Advanced Asperity Models and Persson's Theory. Tribology Letters, 66(2).

Almqvist, A., Campañá, C., Prodanov, N., & Persson, B. N. J., 2011. Interfacial separation between elastic solids with randomly rough surfaces: Comparison between theory and numerical techniques. Journal of the Mechanics and Physics of Solids, 59(11), 2355–2369.

Barthel, E., 2008. Adhesive elastic contacts: JKR and more. Journal of Physics D: Applied Physics, 41(16).

Bradley, R. S. R., 1932. The cohesive force between solid surfaces and the surface energy of solids. The London, Edinburgh, and Dublin Philosophical Magazine and Journal of Science, 13(86), 853–862.

Cheng, W., Dunn, P. F., & Brach, R. M., 2002. Surface roughness effects on microparticle adhesion. Journal of Adhesion, 78(11), 929–965.

Ciavarella, M., Delfine, V., & Demelio, G., 2006. A "re-vitalized" Greenwood and Williamson model of elastic contact between fractal surfaces. Journal of the Mechanics and Physics of Solids, 54(12), 2569–2591.

Ciavarella, M., 2018. A very simple estimate of adhesion of hard solids with rough surfaces based on a bearing area model. Meccanica, 53(1–2), 241–250.

Dening, K., Heepe, L., Afferrante, L., Carbone, G., & Gorb, S. N., 2014. Adhesion control by inflation: implications from biology to artificial attachment device. Applied Physics A, 116(2), 567-573.

Derjaguin, B., 1934. Untersuchungen über die Reibung und Adhäsion, IV - Theorie des Anhaftens kleiner Teilchen. Kolloid-Zeitschrift, 69(2), 155–164.

Derjaguin, B. V., Muller, V. M., & Toporov, Y. P., 1975. Effect of contact deformations on the adhesion of particles. Journal of Colloid And Interface Science, 53(2), 314–326.

Feng, J. Q., 2000. Contact behavior of spherical elastic particles: A computational study of particle adhesion and deformations. Colloids and Surfaces A: Physicochemical and Engineering Aspects, 172(1–3), 175–198.

Feng, J. Q., 2001. Adhesive contact of elastically deformable spheres: A computational study of pull-off force and contact radius. Journal of Colloid and Interface Science, 238(2), 318–323.

Fuller, K. N. G., & Tabor, D., 1975. The Effect of Surface Roughness on the Adhesion of Elastic Solids. Proceedings of the Royal Society A: Mathematical, Physical and Engineering Sciences, 345(1642), 327–342.

Greenwood, J. A., & Williamson, J. B. P., 1966. Contact of Nominally Flat Surfaces. Proceedings of the Royal Society A: Mathematical, Physical and Engineering Sciences, 295(1442), 300–319.

Greenwood, J. A., 1997. Adhesion of elastic spheres. Proceedings of the Royal Society A: Mathematical, Physical and Engineering Sciences, 453(1961), 1277–1297.

Greenwood, J. A., 2006. A simplified elliptic model of rough surface contact. Wear, 261(2), 191–200.

Greenwood, J. A., 2007. On the DMT theory. Tribology Letters, 26(3), 203–211.

He, X., Bai, Q., & Shen, R., 2018. Atomistic perspective of how graphene protects metal substrate from surface damage in rough contacts. Carbon, 130, 672–679.

Hoang, T. V., Wu, L., Paquay, S., Golinval, J. C., Arnst, M., & Noels, L., 2017. A computational stochastic multiscale methodology for MEMS structures involving adhesive contact. Tribology International, 110, 401–425.

Jacobs, T. D. B., Ryan, K. E., Keating, P. L., Grierson, D. S., Lefever, J. A., Turner, K. T., ... Carpick, R. W., 2013. The effect of atomic-scale roughness on the adhesion of nanoscale asperities: A combined simulation and experimental investigation. Tribology Letters, 50(1), 81–93.

Joe, J., Scaraggi, M., & Barber, J. R., 2017. Effect of fine-scale roughness on the tractions between contacting bodies. Tribology International, 111, 52–56.

Johnson, K. L., Kendall, K., & Roberts, A. D., 1971. Surface Energy and the Contact of Elastic Solids. Proceedings of the Royal Society A: Mathematical, Physical and Engineering Sciences, 324(1558), 301–313.

Johnson, K. L., 1985. Contact Mechanics. Journal of the American Chemical Society (Vol. 37).

Maugis, D., 1992. Adhesion of spheres: The JKR-DMT transition using a dugdale model. Journal of Colloid And Interface Science, 150(1), 243–269.

Maugis, D., 1996. On the contact and adhesion of rough surfaces. Journal of Adhesion Science and Technology, 10(2), 161–175.

Medina, S., & Dini, D., 2014. A numerical model for the deterministic analysis of adhesive rough contacts down to the nano-scale. International Journal of Solids and Structures, 51(14), 2620–2632.

Menga, N., Afferrante, L., & Carbone, G., 2016. Adhesive and adhesiveless contact mechanics of elastic layers on slightly wavy rigid substrates. International Journal of Solids and Structures, 88–89, 101–109.

Muller, V. M., Yushchenko, V. S., & Derjaguin, B. V., 1980. On the influence of molecular forces on the deformation of an elastic sphere and its sticking to a rigid plane. Journal of Colloid and Interface Science, 77(1), 91–101.

Muller, V. M., Derjaguin, B. V., & Toporov, Y. P., 1983. On two methods of calculation of the force of sticking of an elastic sphere to a rigid plane.

Colloids and Surfaces, 7(3), 251–259.
Müser, M. H., Dapp, W. B., Bugnicourt, R., Sainsot, P., Lesaffre, N., Lubrecht, T. A., ... Greenwood, J. A., 2017. Meeting the Contact-Mechanics Challenge. Tribology Letters, 65(4).
Pashley, M. D., 1984. Further consideration of the DMT model for elastic contact. Colloids and Surfaces, 12(C), 69–77.
Pastewka, L., & Robbins, M. O., 2014. Contact between rough surfaces and a criterion for macroscopic adhesion. Proceedings of the National Academy of Sciences, 111(9), 3298–3303.
Persson, B. N. J., 2001. Theory of rubber friction and contact mechanics. The Journal of Chemical Physics, 115(8), 3840–3861.
Persson, B. N. J., 2008. On the elastic energy and stress correlation in the contact between elastic solids with randomly rough surfaces. Journal of Physics Condensed Matter, 20(31).
Persson, B. N. J., & Scaraggi, M,. 2014. Theory of adhesion: Role of surface roughness. Journal of Chemical Physics, 141(12).
Putignano, C., Afferrante, L., Carbone, G., & Demelio, G., 2012. A new efficient numerical method for contact mechanics of rough surfaces. International Journal of Solids and Structures, 49(2), 338–343.
Ramakrishna, S. N., Nalam, P. C., Clasohm, L. Y., & Spencer, N. D., 2013. Study of adhesion and friction properties on a nanoparticle gradient surface: Transition from JKR to DMT contact mechanics. Langmuir, 29(1), 175–182.
Rauscher, S. G., Bruck, H. A., & DeVoe, D. L., 2018. Electrical contact resistance force sensing in SOI-DRIE MEMS. Sensors and Actuators, A: Physical, 269, 474–482.
Tabor, D., 1977. Surface forces and surface interactions. Journal of Colloid And Interface Science, 58(1), 2–13.
Violano, G., Demelio, G.P., & Afferrante L., 2018. Adhesion of hard elastic rough bodies with low surface energy. Submitted
Violano, G., & Afferrante L., 2018. On DMT methods to calculate adhesion in rough contacts. Tribology International,130, 36–42.
Wei, Z., He, M. F., & Zhao, Y. P., 2010. The effects of roughness on adhesion hysteresis. Journal of Adhesion Science and Technology, 24(6), 1045–1054.
Yang, C., & Persson, B. N. J., 2008. Contact mechanics: Contact area and interfacial separation from small contact to full contact. Journal of Physics Condensed Matter, 20(21).